

1 **The role of PVP in the bioavailability of Ag from the PVP-stabilized Ag nanoparticle**
2 **suspension**

3

4 Tea Romih^a, Anita Jemec^{a,*}, Monika Kos^a, Samo B. Hočevár^b, Slavko Kralj^c, Darko
5 Makovec^c, Damjana Drobne^a

6

7 ^a Department of Biology, Biotechnical Faculty, University of Ljubljana, Večna pot 111, 1000
8 Ljubljana, Slovenia

9 ^b Analytical Chemistry Laboratory, National Institute of Chemistry, Hajdrihova 19, 1000
10 Ljubljana, Slovenia

11 ^c Department for the Synthesis of Materials, Jožef Stefan Institute, Jamova 39, 1000
12 Ljubljana, Slovenia

13

14

15 ***Corresponding author:**

16 Anita Jemec

17 University of Ljubljana

18 Biotechnical Faculty, Department of Biology

19 Večna pot 111

20 1000 Ljubljana

21 Slovenia

22 Phone: +386 1 320 33 75

23 Fax: +386 1 257 33 90

24 E-mail: anita.jemec@bf.uni-lj.si

25 **ABSTRACT**

26 We assessed the bioavailability of Ag from Ag nanoparticles (NPs), stabilized with
27 polyvinylpyrrolidone (PVP), to terrestrial isopods which were exposed to 10, 100 and 1000
28 μg Ag NPs/g of dry food. Different Ag species were determined in the NP suspension that
29 was fed to isopods: (i) total Ag by atomic absorption spectroscopy, (ii) the sum of Ag-PVP
30 complexes and free Ag^+ by anodic stripping voltammetry at the bismuth-film electrode, and
31 (iii) free Ag^+ by ion-selective potentiometry. The amounts of Ag species in the consumed
32 food were compared to the masses of Ag accumulated in the isopod digestive glands. Our
33 results show that all three Ag species (Ag NPs, Ag-PVP complexes and free Ag^+) could be the
34 source of bioaccumulated Ag, but to various degrees depending on the exposure concentration
35 and transformations in the digestive system. We provide a proof that (i) Ag NPs dissolve and
36 Ag-PVP complexes dissociate in the isopod digestive tract; (ii) the concentration of free Ag^+
37 in the suspension offered to the test organisms is not the only measure of bioavailable Ag. The
38 type of NP stabilizer along with the NP transformations in the digestive system needs to be
39 considered in the creation of new computational models of the nanomaterial fate.

40

41 **KEYWORDS:** Ag ions, Ag complexes, voltammetry, ion-selective electrode, terrestrial
42 isopod

43

44 **HIGHLIGHTS:**

- 45 • Ag from Ag NPs, Ag-PVP complexes and free Ag^+ accumulates in isopod hepatopancreas.
46 • Ag NPs dissolve in the digestive tract of terrestrial isopods.
47 • Ag-PVP complexes dissociate in the digestive tract of terrestrial isopods.
48 • NP stabilizer affects the bioavailability of metals from metal NPs.

49 *CAPSULE: The polyvinylpyrrolidone stabilizer for Ag NPs forms labile complexes with Ag⁺,*
50 *which are bioavailable to the test terrestrial isopod.*

51

52 **INTRODUCTION**

53 In the recent years, it has been recognized that nanoparticles (NPs) can undergo a
54 number of transformations such as agglomeration/aggregation, surface association with
55 organic molecules, dissolution, and the formation of corona on their surface (Lowry et al.,
56 2012). These processes govern the bioavailability, cellular internalization and toxicity of NPs.
57 At present, it is believed that ions dissolved from NPs are among the main mediators of their
58 biological effects on organisms (Ivask et al., 2014). Organisms can either increase the
59 dissolution of metal/metal oxide NPs (for example Ag NPs, Cu NPs, CoFe₂O₄ NPs and rare-
60 earth oxide NPs; Golobič et al., 2012; Bondarenko et al., 2013; Novak et al., 2013; Huynh et
61 al., 2014; Leclerc and Wilkinson, 2014; Diez-Ortiz et al., 2015; He et al., 2015; Romih et al.,
62 2015) or decrease their dissolution (for example aminosilane-capped ZnO quantum dots;
63 Bellanger et al., 2015). In the case of bacteria and unicellular algae, the NP dissolution takes
64 place outside the organism at the point of contact with NPs (Bondarenko et al., 2013; Huynh
65 et al., 2014; Leclerc and Wilkinson, 2014; Bellanger et al., 2015; He et al., 2015) while in the
66 case of isopods and earthworms, the NP dissolution is suggested to occur inside the digestive
67 tract in contact with digestive juices (Golobič et al., 2012; Novak et al., 2013; Diez-Ortiz et
68 al., 2015; Romih et al., 2015).

69 Terrestrial isopods (e.g. *Porcellio scaber*, *Porcellionides pruinosus*) have become
70 established model organisms for metal kinetics and metal nanoparticle transformations
71 (Romih et al., 2015; Tourinho et al., 2015, 2016). Focus is set in particular on digestive gland
72 (hepatopancreas), which is the main digestive and metal storage organ (Hames and Hopkin,
73 1989). The advantage of this test model is an almost exclusive uptake of NPs through oral

74 route and negligible surface uptake (Vijver et al., 2005), which enables the determination of
75 exact metal mass balances. In our previous studies with isopods *P. scaber* (Golobič et al.,
76 2012; Novak et al., 2013; Romih et al., 2015), we have provided the first evidence that
77 digestive juices enhance the dissolution of selected metal/metal oxide NPs inside the
78 organism. In the study with Cu NPs (Golobič et al., 2012), no particle stabilizers were present
79 and the net bioaccumulation of dissolved ions showed an enhanced dissolution of NPs in the
80 digestive system. In the studies with either bare or citric acid-adsorbed CoFe₂O₄ NPs (Novak
81 et al., 2013; Romih et al., 2015), we additionally showed that citric acid enhances the
82 dissolution of NPs in the suspension, but decreases the bioavailability of dissolved metal ions
83 due to chelation at the near-neutral pH of the *P. scaber* digestive system.

84 To advance our understanding of NP transformations within the digestive system of
85 isopods and the role of NP stabilizer in the bioavailability of dissolved metals, we performed
86 a study with Ag NPs stabilized with polyvinylpyrrolidone (PVP). Silver NPs are most
87 commonly stabilized with PVP, which is known to form weak coordinative bonds with Ag⁺
88 (Zhang et al., 1996; Wang et al., 2005). Suspensions of PVP-stabilized Ag NPs therefore
89 contain at least three different Ag species: Ag⁰ (Ag NPs), Ag-PVP complexes and free Ag⁺.
90 To the best of our knowledge, the stability constant of Ag-PVP complexes has not been
91 determined yet and the behavior of these complexes in relation to, for example, pH, ionic
92 strength and temperature, is unknown. It is also unknown how Ag-PVP complexes behave in
93 the digestive system of organisms. The bioavailability (as defined by Riding et al., 2013) of
94 Ag from PVP-stabilized Ag NPs therefore cannot be predicted in advance; both biological and
95 chemical means are needed to elucidate the dynamic processes taking place inside the isopod
96 digestive system.

97 In our previous studies (Golobič et al., 2012; Novak et al., 2013), the amount of free
98 ions in NP suspensions used to spike the food was quantified by the ultracentrifugation

99 approach coupled with spectrometry. This approach has been one of the most commonly
100 applied in metal/metal oxide NP dissolution analyses, but it has been criticized in terms of
101 incomplete discrimination between ions and particulate matter (Misra et al., 2012; Tantra et
102 al. 2015; Jemec et al., 2016). Namely, spectroscopic techniques may overestimate the amount
103 of free metal ions if the separation between ions and particulate matter is not efficient (Jemec
104 et al., 2016). The novelty of the study presented herein is that electrochemical techniques,
105 such as potentiometry using ion-selective electrodes (ISEs), and anodic stripping voltammetry
106 (ASV), were used to determine the share of free ions and their complexes in the suspension of
107 Ag NPs added to food. These two techniques have been previously recommended (Tantra et
108 al. 2015; Romih et al., 2015, 2016). Anodic stripping voltammetry and potentiometry differ in
109 the metal species they detect: while potentiometry is used for detecting only free ions, the
110 ASV can be exploited for measuring both free ions and labile ion-ligand complexes. Anodic
111 stripping voltammetry offers an advantage over the potentiometric approach as it enables the
112 measurements of a much wider selection of elements and is significantly more sensitive, i.e.
113 enables lower detection limits (Pesavento et al., 2009). The complementary data from
114 potentiometric measurements (for Ag, Cu and Pb) and ASV measurements provide valuable
115 information on metal speciation in the suspensions of the corresponding NPs.

116 The aim of this study was to assess the bioavailability of Ag for *P. scaber* when
117 offered as a composite Ag NP suspension stabilized with PVP as a surfactant, which was not
118 chemically attached to the NP surface as a coating, but was added to suspension as a
119 surfactant creating sterical hindrance among NPs. The suspension consisted of Ag NPs, Ag-
120 PVP complexes and free Ag⁺. For this purpose, we first quantified the three Ag species in the
121 suspension applied to the food that was offered to isopods, and compared them to the amount
122 of Ag accumulated in the digestive glands. Due to transformations of Ag in the digestive
123 system and the presence of PVP, which could additionally affect the Ag bioavailability, the

124 question was whether more free ions as ingested are available for the bioaccumulation or less.
125 If Ag^+ form weak complexes with PVP, which dissociate under physiological conditions, we
126 expect Ag from Ag-PVP complexes to be bioavailable. On the other hand, if Ag-PVP
127 complexes dissociate to a limited extent, we do not expect them to provide a source for Ag
128 accumulation. We discuss the role of PVP as a stabilizing agent for Ag NPs and its effect on
129 the bioavailability of Ag for isopods.

130

131 **EXPERIMENTAL**

132 *Silver nanoparticle sample preparation and characterization*

133 Silver NPs (designated as NNV 003; batch number Parnasos_IG010305_Ag
134 NAMA39_1202_Ag) were supplied by the Colorobbia S.p.A. (Firenze, Italy) within the
135 framework of the EU FP7 NanoValid project. The Ag NPs were supplied as an aqueous
136 suspension with nominal particle concentration 40 g/L, stabilized with PVP as a surfactant
137 which was added into the suspension (not chemically attached to the NP surface). The data on
138 particle size, shape, and ζ -potential was provided by the partners of the EU FP7 NanoValid
139 project. The exact concentration of the PVP stabilizer is considered an intellectual property of
140 the supplier and could not be revealed.

141 The stock suspension of Ag NPs was diluted with deionized water (MilliQ, Millipore,
142 Bedford, Massachusetts, USA [$\rho = 18.5 \text{ M}\Omega\cdot\text{cm}$]), prior to the use in experiments. For the
143 dissolution measurements we chose the concentrations 12.5, 25 and 50 mg/L of Ag, which are
144 lower than those applied on the leaves (10, 100 and 1000 mg/L). The reason was that PVP in
145 the very same Ag NP suspension had been shown to interfere with the silver ion-selective
146 electrode (Ag-ISE) already at the concentration 25 mg/L (Romih et al., 2016). The total Ag
147 contents in the diluted Ag NP suspensions were checked with flame AAS after overnight
148 digestion in 1 M HNO_3 (suspension/acid ratio 1:1 vol/vol).

149 ***Silver nanoparticle dissolution measurements***

150 Eight milliliters of diluted suspensions at concentrations 12.5, 25 and 50 mg/L of Ag
151 were ultracentrifuged in duplicate at 100 000 g for 30 min at 20 °C (Beckman Coulter L8-
152 70M class H preparative ultracentrifuge with Type 70.1 Ti rotor and 10 mL thickwall
153 polyallomer tubes). The supernatants were then divided into two aliquots for Ag
154 quantification. The first aliquot was acidified with 65 % HNO₃ (analytical grade purity;
155 Fischer Scientific, Leicester, UK) and the total Ag content was quantified by flame AAS. The
156 second aliquot was left unacidified and was used for the determination of the Ag species (the
157 sum of Ag-PVP complexes and free Ag⁺) by ASV and free Ag⁺ by potentiometry with Ag-
158 ISE. The stock suspension was also measured by ASV without prior ultracentrifugation or
159 acidification; the measurements were carried out in the same way as for the supernatants of
160 the diluted suspensions. The unacidified supernatants were checked for the presence of
161 unsedimented NPs by the dynamic light scattering (DLS) measurements using Analysette 12
162 DynaSizer (Fritsch GmbH, Idar-Oberstein, Germany). All the characterization steps were
163 performed on freshly-prepared suspensions.

164 The ASV approach followed the newly-developed protocol, which was described in
165 Romih et al. (2016). The measurements were performed using the PalmSens
166 potentiostat/galvanostat (PalmSens BV, Utrecht, Netherlands) in combination with the
167 PSTrace 4.4 software (PalmSens BV). The usual three-electrode configuration was employed
168 with the bismuth electrode prepared *in-situ* on a glassy carbon (GCE) disk (d = 2 mm) as the
169 working electrode, a platinum wire as the counter electrode, and a double-junction saturated
170 Ag/AgCl/KCl reference electrode containing 0.1 M HNO₃ as the outer electrolyte to prevent
171 chloride leakage into the sample solution. A computer-controlled magnetic stirrer, rotating at
172 approximately 300 rpm, was employed during the electrochemical accumulation step. All
173 experiments were carried out at room temperature of 23±1 °C in a 20 mL one-compartment

174 voltammetric cell. The standard solutions of bismuth(III) and silver(I) were provided by
175 Merck (Darmstadt, Germany) and further diluted as required. 0.1 M acetate buffer solution
176 with pH 4.5 was used as a supporting electrolyte. Water used throughout the work was first
177 deionized and then further purified using Elix 10/Milli-Q Gradient unit (Millipore, Bedford,
178 Massachusetts, USA). Following an electrochemical accumulation step of 60 s at -0.8 V, and
179 a subsequent equilibration period of 15 s, an anodic stripping voltammogram was recorded in
180 a quiescent solution by scanning the potential towards more positive values using a square-
181 wave potential scan from -0.6 V to $+0.6$ V vs. the reference electrode, with a frequency of 25
182 Hz, a potential step of 4 mV, and an amplitude of 50 mV. Before each measurement, a
183 cleaning step was carried out by applying the potential of $+0.4$ V for 30 s.

184 The potentiometric measurements were performed using the perfectION™ Ag/S₂
185 combination ion-selective electrode (Mettler Toledo, Greifensee, Switzerland). The
186 experiments were carried out at room temperature of 23 ± 1 °C in a 20 mL beaker with the use
187 of a magnetic stirrer rotating at 300 rpm. The ionic strength adjustment solution
188 (perfectION™ Ion Electrolyte B, Mettler Toledo) was added to the samples following the
189 protocol of the supplier (ionic strength adjustment solution : sample ratio = 1:50 vol/vol). The
190 Ag-ISE was submerged in the sample after adding the ion strength adjustment solution. The
191 electrode potential was recorded after equilibration for at least two minutes.

192 The concentrations of free Ag⁺ and Ag-PVP complexes in the supernatants of the Ag
193 NP suspensions were determined by the method of three standard additions (Harris, 2010).

194

195 ***Feeding experiment with terrestrial isopods Porcellio scaber***

196 Terrestrial isopods *P. scaber* were collected in September of 2013 from a compost
197 heap in a non-polluted garden in Podutik, Ljubljana, Slovenia. Animals were kept in a climate
198 chamber at 22 ± 1 °C with a 16/8 h light/dark period (120 and 16 lx, respectively; measured

199 using LI-1000 Data Logger, LI-COR, Nebraska, USA), caged in glass containers with moist
200 loamy sand and peat at the bottom. They were fed dry fallen common hazel leaves (*Corylus*
201 *avellana*) for three weeks before the Ag exposure. *P. scaber* adults of both sexes, including
202 those at the intermoult and early premoult stages (Zidar et al., 1998) and weighing between 30
203 and 70 mg of fresh body mass, were selected for the experiments. Moulting individuals (Zidar
204 et al., 1998) and gravid females were excluded.

205 The experimental setup was performed as described previously (Romih et al., 2015).
206 During the experiment, the animals were fed dry common hazel leaves that were spiked with
207 deionized water (MilliQ, Millipore, Bedford, Massachusetts, USA) as the negative control,
208 AgNO₃ (≥99.5 % trace metals basis, Sigma Aldrich, Steinheim, Germany) as the dissolved
209 ion control, and Ag NPs as the experimental compound. All of the test chemicals were
210 prepared freshly prior to the experiment at concentrations of 10, 100, and 1000 mg Ag/L. 100
211 μL of a test chemical per 100 mg of leaf was applied onto abaxial leaf surfaces with a pipette
212 and spread evenly with a paintbrush (Giotto, F.I.L.A. S.p.A., Pero, Italy), which resulted in
213 the nominal exposure concentrations of 10, 100, and 1000 μg Ag/g of dry leaf mass. The
214 concentrations were chosen on the basis of the work of Pipan-Tkalec et al. (2011), where no
215 adverse effects of Ag NPs on *P. scaber* in terms of feeding rate or body mass change were
216 found in the range of exposure concentrations at 0.1–5000 μg/g of dry food. The leaves were
217 left to dry at room temperature and were re-weighed prior to the experiment. The animals
218 were weighed and placed individually into plastic Petri dishes (∅ = 9 cm) along with the
219 prepared leaves with the contaminated side facing up. No soil or other substrate was added.
220 Each exposure group contained 15 animals; there were no significant differences in the
221 distributions of fresh body masses among the animals divided into different test groups
222 ($p > 0.05$, Mann-Whitney *U*-test, results not shown). The experiment was maintained for 14
223 days in controlled and stable conditions at 22±1 °C, 80 % relative humidity (TFA Dostmann

224 GmbH & Co.KG, Wertheim, Germany), with a 16/8 h light/dark period (120 and 16 lx,
225 respectively) and monitored on a daily basis. The humidity in the Petri dishes was maintained
226 by periodical spraying of deionized water on the internal sides of the lids. At the end of the
227 experiment, the animals were switched to uncontaminated hazel leaves for 1 day to deplete
228 the Ag-spiked food from their digestive systems. The uneaten spiked leaves were collected,
229 air-dried and weighed. Fecal pellets were also weighed after drying in a desiccator for 24 h.
230 After the depuration period, animal mortality was recorded and the surviving animals were
231 weighed. The animals were decapitated and their digestive glands were isolated. Individual
232 digestive glands were placed on small pieces of filter paper (approximately 4 mm × 7 mm in
233 size), stored in plastic tubes, and frozen at -20 °C until further analyses.

234 A sample of fecal pellets was attached to aluminum holders with a double-sided
235 adhesive carbon tape and inspected for the presence of NPs with a thermal field-emission
236 scanning electron microscope (JEOL JSM-7600F, Tokyo, Japan) under the accelerating
237 voltage of 15 kV (**Supplementary Figures S8–S11**).

238

239 *Measurements of metal content in food and in the animal tissues*

240 The total Ag concentration in the digestive glands of isopods and in the uneaten leaf
241 remnants after the experiments was determined by flame AAS. Prior to the analysis, the
242 samples were acid digested in concentrated nitric acid (65 % HNO₃, analytical grade purity,
243 Fisher Scientific, Loughborough, UK) in the Milestone Ethos E microwave lab station
244 (Milestone, Bergamo, Italy) equipped with a SK-10 high pressure segmented rotor and 3 mL
245 quartz microsampling inserts. Digestion was conducted at 180°C and 600 W power, with step
246 1 (heating) lasting 15 min, step 2 (constant temperature) lasting 10 min, and 45 min cooling to
247 60 °C.

248

249 ***Data analyses of feeding parameters and metal concentrations***

250 The animals that died during moulting and gravid females were excluded from further
251 data processing (n = 19 in total). The numbers of analyzed animals are presented in the
252 figures as part of the x-axis labels. The data are presented as mean values, and uncertainties
253 are expressed as standard deviations (SD). All the data shown in the figures describe nominal
254 concentrations of Ag (10, 100, and 1000 µg/g of dry leaf). The statistical significances of the
255 differences between the control and exposed groups of animals were assessed by the Mann-
256 Whitney *U*-test (* $p < 0.05$, ** $p < 0.01$, *** $p < 0.001$) using the OriginPro 8.0 software
257 (OriginLab Corp., Northampton, MA, USA). The formulae for all the calculations used in the
258 present study (the shares of Ag-PVP complexes and free Ag⁺ that dissolved from the
259 nanoparticles, the masses of Ag consumed by the isopods and the shares of Ag accumulated
260 into their digestive glands upon exposure to Ag) are provided in the **Supplementary**
261 **Material as Equations (S1) to (S4).**

262

263 **RESULTS**

264 ***Silver nanoparticle characteristics***

265 Silver NPs were supplied as an aqueous suspension with a nominal particle
266 concentration of 40 g/L (the mean measured total Ag concentration was 41.14 g/L; Jemec et
267 al., 2016). The same batch of Ag NPs has been previously characterized and described in Zou
268 et al. (2015), Böhme et al. (2015) and Jemec et al. (2016). In summary, the mean primary
269 particle size of the NPs was 20±7 nm (transmission electron microscopy), and the
270 hydrodynamic diameter in deionized water was 116±7 nm (dynamic light scattering). The ζ-
271 potential of Ag NPs was -19±9 mV.

272

273 *Concentrations of total Ag in suspensions applied onto leaves and concentrations of Ag on*
274 *the leaves after the experiment*

275 The actual measured concentration of total Ag in the suspensions used for the
276 dissolution measurements (10.6 ± 0.1 , 20.9 ± 0.9 and 44.9 ± 1.1 mg/L; **Table 1**) differed from
277 their corresponding nominal values (12.5, 25 and 50 mg/L, respectively) within a 20 % range.
278 The actual measured concentrations of total Ag on the AgNO₃-spiked and Ag NP-spiked
279 leaves (6.5 ± 0.6 , 79 ± 33 and 914 ± 38 μg/g of dry leaf mass in the case of AgNO₃; 6.1 ± 2.9 ,
280 65 ± 7 and 956 ± 68 μg/g of dry leaf mass in the case of Ag NPs; **Table S1, Supplementary**
281 **Material**) were slightly lower than their corresponding nominal values (10, 100 and 1000
282 μg/g of dry leaf mass, respectively, for both compounds). Low recovery is a consequence of
283 losses during pipetting due to high viscosity of the Ag NP suspension. Only actual measured
284 values were used in all the calculations.

285

286 *Concentrations of Ag-PVP complexes and free Ag⁺ in the Ag NP suspensions*

287 After the ultracentrifugation of the Ag NP suspensions at nominal concentrations of
288 12.5, 25 and 50 mg/L of total Ag, the supernatants were measured by flame AAS, ASV using
289 bismuth-film electrode, and potentiometry using Ag-ISE. The flame AAS measurements
290 denote the concentration of total Ag (free Ag ions, Ag-PVP complexes, unsedimented Ag
291 NPs), ASV values denote the sum of free Ag⁺ and Ag-PVP complexes, and potentiometric
292 measurements denote free Ag⁺ only.

293 The flame AAS yielded higher values than both other methods, i.e. ASV and
294 potentiometry (**Table 1**), denoting uncomplete sedimentation of NPs during
295 ultracentrifugation. This was corroborated by the dynamic light scattering analysis, which
296 revealed the presence of particles with hydrodynamic diameters of ≥ 70 nm in the supernatants
297 (**Figures S1–S3, Supplementary Material**).

298 The ASV measurements (**Table 1**) showed that the supernatants contained 42–47 % of
299 the free Ag⁺ and Ag-PVP species in total (depending on the nominal concentration of Ag
300 NPs). We also measured the non-centrifuged stock suspension, and the share of Ag-PVP
301 complexes and free Ag⁺ in comparison to the total Ag was 44±3 % (n = 3).

302 The free Ag⁺ content values yielded by the potentiometric measurements were lower
303 than those yielded by ASV, showing the presence of 27, 12 and 12 % of free Ag⁺ in the case
304 of 12.5, 25 and 50 mg/L nominal concentrations of Ag NPs, respectively (**Table 1**). The
305 potentiometry, i.e. Ag-ISE, showed unexpectedly deviant behavior at the highest
306 concentration (50 mg/L), as evident from its non-linear response (**Figures S4 and S5,**
307 **Supplementary Material**). The value obtained at this concentration therefore represents an
308 approximation. The values obtained at the lower two concentrations (12.5 and 25 mg/L) are
309 considered accurate, because the electrode response was linear and the slope remained at
310 approximately 80 % of the ideal value (**Figures S4 and S5, Supplementary Material**).

311 *Please insert Table 1 here.*

312

313 ***Concentrations of Ag in isopod digestive glands***

314 To evaluate the potential of terrestrial isopods to accumulate Ag from an Ag NP
315 suspension containing various Ag species (Ag NPs, Ag-PVP complexes and free Ag⁺), a
316 feeding experiment with *P. scaber* was performed. After feeding for 14 days on Ag-spiked
317 leaves, the animals from all the exposure groups contained significantly more Ag in their
318 digestive glands than the animals from the control group ($p < 0.05$ and $p < 0.001$, **Figure 1**).
319 However, there were no statistical differences between the animals exposed to different
320 sources of Ag (AgNO₃ or Ag NPs) at same exposure concentrations ($p > 0.05$, not marked on
321 **Figure 1**).

322

323 *Please insert Figure 1 here.*

324

325 ***Comparison of the consumed Ag species (Ag NPs, Ag-PVP complexes and free Ag⁺) and***
326 ***the bioaccumulated Ag in isopod digestive glands***

327 Data for the consumed amounts of different Ag species and the amount of
328 bioaccumulated Ag in *P. scaber* digestive glands is presented in **Table S1 (Supplementary**
329 **Material)**. Based on this data we compared the masses of Ag found in the hepatopancreas
330 after the experiment to the masses of each ingested Ag species following the approach of
331 Romih et al. (2015) in order to elucidate which ingested Ag species may be potential sources
332 of bioaccumulated Ag (**Figures 2a-c**). At the exposure concentration of 10 µg Ag/g of dry
333 food, the amount of bioaccumulated Ag was much higher than the amount of consumed free
334 Ag⁺ (**Figure 2a**). At the exposure concentration of 100 µg Ag/g of dry food, the amount of
335 bioaccumulated Ag was also higher than the consumed amount of free Ag⁺, although this
336 difference was not as pronounced as in the case of 10 µg Ag/g of dry food (**Figure 2b**). At the
337 exposure concentration of 1000 µg Ag/g of dry food, the amount of bioaccumulated Ag was
338 lower than the ingested amounts of any of the Ag species (**Figure 2c**).

339

340 *Please insert Figure 2 here.*

341

342 ***Effects of AgNO₃ and Ag NPs on isopod food consumption***

343 The feeding rate of isopods exposed to 10 µg Ag/g of dry food either in the form of AgNO₃ or
344 Ag NPs, as well as the feeding rate of isopods exposed to 100 µg Ag/g of dry food in the form
345 of Ag NPs did not significantly differ from the control group (**Figure S6**; $p > 0.05$, Mann-
346 Whitney U-test). The feeding rates of isopods exposed to AgNO₃ at the exposure
347 concentrations 100 and 1000 µg Ag/g of dry food, and to the Ag NPs at the exposure

348 concentration 1000 µg Ag/g of dry food were significantly lower than the feeding rate in the
349 control group (**Figure S6**; Mann-Whitney U-test, * $p < 0.05$, ** $p < 0.01$ and * $p < 0.05$,
350 respectively).

351

352 **DISCUSSION**

353 In the present study, we used two analytical methods, i.e. ASV and potentiometry with
354 Ag-ISE, to measure the Ag speciation in suspensions of commercial PVP-stabilized Ag NPs
355 applied to food, and the data on Ag bioaccumulation in digestive gland with the aim to
356 elucidate which Ag species (Ag NPs, Ag-PVP complexes, free Ag⁺) in the Ag NP suspension
357 could be the potential source of Ag that was accumulated by the isopods. We provide an
358 indirect proof of the dissolution of Ag NPs in the presence of PVP and the dissociation of Ag-
359 PVP complexes in the digestive system of terrestrial isopods *P. scaber*, which will be
360 discussed below.

361

362 *Analytical approaches to discriminate among different Ag species in the PVP-stabilized Ag* 363 *NP suspension*

364 We applied three different approaches to identify different Ag species in the Ag NP
365 suspension: the commonly employed flame AAS coupled with ultracentrifugation, ASV
366 measurements of Ag at the *in-situ* prepared bismuth film electrode following the recently
367 developed protocol (Romih et al., 2016) and potentiometry using the commercial Ag-ISE.

368 Flame AAS yielded higher values of Ag than both other methods (**Table 1**). This was
369 corroborated by the dynamic light scattering analysis of the supernatants, which revealed the
370 presence of unsedimented particles (**Figures S1–S3, Supplementary Material**). Our results
371 are in line with other reports, which state that ultracentrifugation coupled with spectroscopic
372 determination cannot distinguish among free ions, ion-ligand complexes and unsedimented

373 NPs (Misra et al., 2012; Tantra et al. 2015), unless ultracentrifugation is performed at very
374 high speeds and long durations (for example 362 769 g for 1 h) where complete NP
375 sedimentation is possible (Jemec et al., 2016). However, maximum ultracentrifugation speeds
376 and centrifugal forces depend on the type of centrifuge, rotor and tubes (Beckman Coulter,
377 2007). The centrifugal force reported in Jemec et al. (2016) is not universally attainable and
378 alternative approaches to the ultracentrifugation coupled with spectroscopy are preferable.

379 We were able to discriminate between Ag NPs and the sum of Ag-PVP complexes and
380 free Ag⁺ in the supernatants after ultracentrifugation as well as in the non-centrifuged stock
381 suspension by the ASV at the *in-situ* prepared bismuth film electrode. The values (in the
382 range of 44–48 %; **Table 1**) were consistent with the previously reported values for the same
383 Ag NP stock (46 %; Jemec et al., 2016).

384 As expected, the contents of free Ag⁺ only, measured by the Ag-ISE, were lower (27
385 %, 12 % and 12 %) than the values recorded by the ASV (**Table 1**). However, we observed
386 atypical behavior of the Ag-ISE, which was presumably caused by PVP that became adsorbed
387 on the electrode and obstructed the access of free Ag⁺ to the sensor surface. The deviations
388 from linearity and/or the decrease of the electrode slope were more pronounced with
389 increasing concentrations of Ag NPs (**Figures S4 and S5, Supplementary Material**). Similar
390 interferences from organic molecules when measuring samples with complex matrices are
391 well-known in ion-selective potentiometry (De Marco et al., 2007; Dimeski et al., 2010).
392 Although ISEs might be attractive for the purpose of measuring free ion content in NP
393 suspensions due to low cost, fast response, preservation of the sample and no requirements for
394 extensive operator training (Koch et al., 2012; Tantra et al., 2015), the interferences due to
395 organic molecules demonstrate that potentiometry is not the method of choice with complex
396 samples. In this case, a better option is the voltammetric counterpart of ion-selective

397 potentiometry, the Absence of Gradients and Nernstian Equilibrium Stripping (AGNES)
398 technique (Domingos et al., 2013, 2015; Mu et al., 2014; Merdzan et al., 2014).

399 *Transformations of Ag NPs in the isopod digestive system and the bioavailability of Ag*
400 *from the PVP-stabilized Ag NP suspension*

401 In this study we assumed that only free Ag⁺, and not Ag NPs, are accumulated in the
402 isopod digestive glands. This assumption was based on the previously published work by
403 Pipan-Tkalec et al. (2011), Novak et al. (2013), and Tourinho et al. (2016). Namely, when the
404 digestive glands of the NP-fed isopods were inspected by the elemental composition imaging
405 techniques, such as proton-induced X-ray emission (PIXE) or synchrotron X-ray fluorescence
406 microscopy (μ XRF), the NP-originating metals (i.e. Ag and Co) were found associated
407 exclusively with the S-cells of the hepatopancreas (Pipan-Tkalec et al., 2011; Novak et al.,
408 2013; Tourinho et al., 2016). The S-cells are a bioaccumulation site for metal ions with the
409 affinity for sulphur-bearing ligands (Hopkin, 1990). Moreover, only Co and not Fe was
410 accumulated into hepatopancreatic cells from the composite CoFe₂O₄ NPs, which indicates
411 that NPs were not internalized intact (Novak et al., 2013).

412 Our results show that the amount of accumulated Ag in digestive glands at the two
413 lower exposure concentrations (10 and 100 μ g Ag/g of dry food), was higher than the amount
414 of consumed free Ag⁺, which means that only free Ag⁺ were not sufficient to explain the
415 amount of Ag accumulated by the isopods (**Figure 2a,b**). We therefore suggest that the
416 remaining Ag must have both dissolved from Ag NPs and dissociated from Ag-PVP
417 complexes. We think that neither of these two Ag species alone (Ag NPs or Ag-PVP
418 complexes) could be a sufficient source of Ag, because it would mean that Ag assimilation
419 efficiency from any of the two Ag sources had to be very high (>80 %). This, however, is
420 physiologically unrealistic (Zidar et al., 2003). For example, the metal assimilation efficiency
421 of *P. scaber* did not exceed 5 % for Co from Co(NO₃)₂ (Drobne and Hopkin, 1994) and ~60

422 % for Cd from CdCl₂ (Zidar et al., 2003) at similar exposure concentrations in a similar
423 exposure setup as used in the current study. Moreover, Ag NPs could not provide the only
424 source of remaining Ag, because undissolved NPs were found in the fecal pellets after the
425 feeding experiment (albeit in very small quantities; **Figures S8–S11, Supplementary**
426 **Material**).

427 Our results therefore show that Ag-PVP complexes were able to dissociate under
428 physiological conditions, although the near-neutral pH in the digestive system of *P. scaber*
429 (Zimmer & Topp, 1997; Zimmer & Brune, 2005) is generally unfavorable for the dissociation
430 of metal-ligand complexes. The facile release of Ag⁺ from PVP was most likely permitted by
431 weak coordinative bonds between the C–N and C=O functional groups of PVP and the *sp*
432 orbitals of Ag⁺ (Zhang et al., 1996; Wang et al., 2005). The complexation of PVP with Ag⁺
433 and the bioaccessibility of Ag⁺ from Ag-PVP complexes could be further supported with
434 additional Ag accumulation experiments where isopods would be exposed to Ag-salt and
435 selected concentrations of PVP. However, in this particular study, we were unable to elucidate
436 the concentration and molecular weight of the PVP added to the Ag NP suspension, because
437 the producer considers it intellectual property. Another way would be the characterization of
438 PVP in the Ag NP suspension, but this exceeds the scope of this study. We suggest that such
439 studies are carried out in the future using different NP stabilizing agents.

440 At the highest exposure concentration (1000 µg Ag/g of dry food), the amount of
441 ingested free Ag⁺ was higher than the amount of accumulated Ag, which means that free Ag⁺
442 only could be a sufficient source of accumulated Ag (**Figure 2c**). However, this does not
443 exclude the possibility that also at this concentration Ag NPs and Ag-PVP complexes
444 dissolved or dissociated in the gut, respectively. We speculate that the tendency of Ag NPs to
445 dissolve at this concentration was less pronounced than at the lower two exposure
446 concentrations, because the amount of accumulated Ag in the case of Ag NP exposure was

447 significantly lower ($p < 0.01$, Mann-Whitney U -test) than in the case of the same Ag
448 concentration of AgNO₃ (**Table S1, Supplementary Material**). The isopods exposed to Ag
449 NPs could potentially accumulate as much Ag as the case of AgNO₃ (which is considered the
450 physiological storage capacity of *P. scaber* for Ag), but for some reason this did not occur.
451 Most probably, this was due to limited bioavailability of Ag from Ag NPs under given
452 experimental conditions. The lower dissolution of Ag NPs at higher concentration is in line
453 with the data which indicate that Ag NP dissolution in aqueous suspension is inversely related
454 to the NP concentration (Jemec et al., 2016).

455

456 *Transformations of the Ag NP suspension after drying on the test leaves*

457 After drying of the Ag NP suspension on the leaf surface, the share of each Ag species
458 probably does not exactly equal those measured in the aqueous suspension before application.
459 We assume that possible transformations of the Ag NP suspension on the leaves during drying
460 are: (i) the complexation of Ag⁺ to either PVP or Ag NPs, (ii) adsorption/binding of all Ag
461 species to the leaf surface, and (iii) the aggregation/agglomeration of Ag NPs, which may in
462 turn affect the dissolution (Coutris et al., 2012; Schaumann et al., 2015; Tourinho et al.
463 2015). All these transformations result in less free Ag⁺ potentially available for assimilation
464 than those measured in the suspensions applied onto leaves, which further supports the main
465 conclusion of this work. Namely, the dissolution of Ag NPs is lower in the case of larger NP
466 aggregates (Schaumann et al., 2015). Also, AgNO₃ and Ag NPs have previously been shown
467 to bind to soil particles (Coutris et al., 2012), which may also be the case for leaves. We
468 measured the amount of total Ag on the leaves after drying. Measured Ag concentrations in
469 the case of Ag NPs were lower than the nominal value as applied with the suspension.
470 However, this was the case also for AgNO₃, which means that the difference between nominal
471 and measured concentrations was due to spiking accuracy and not due to NPs falling off the

472 leaves. PVP is not volatile, therefore we presume that the amount of PVP in the suspension
473 before and after spiking the leaves was similar.

474 Another potential transformation of Ag NP suspension on leaves may be due to aging
475 of Ag NPs during the 14 days of exposure. It has been previously shown that the tested Ag NP
476 suspension is stable in terms of dissolution and hydrodynamic size (up to a year in stock
477 suspension at 8 °C, and up to 96 h in aqueous suspension at room temperature; Jemec et al.,
478 2016). Shoults-Wilson et al. (2011) studied the speciation of PVP-stabilized Ag NPs in soil
479 during 28 days. They reported that most of the silver remained as Ag⁰, and only partial
480 oxidation of Ag NPs has been found. However, it is unclear how the light exposure may
481 transform the Ag NPs on the leaves.

482 Nevertheless, since the characterization of different Ag species on leaves requires
483 complex techniques and is commonly not feasible, similarly as in the case of soil (Coutris et
484 al., 2012; Schaumann et al., 2015), the characterization in the suspension prior to addition on
485 leaves may currently be the best approximation.

486

487 ***Effects of AgNO₃ and Ag NPs on isopod food consumption***

488 The feeding rates of isopods exposed to Ag NPs (1000 µg Ag/g of dry food) were
489 significantly lower than the feeding rate in the control group. This was also reported for
490 terrestrial isopods *Porcellionides pruinosus* fed on Ag NP-contaminated soil for 14 days
491 (EC50 value 127 [56.4–200] µg Ag/g of dry soil; Tourinho et al., 2015). However, no effect
492 on *P. scaber* fed on Ag NPs (up to 5000 µg Ag/g) for 14 days was noted by Pipan-Tkalec et
493 al. (2011). This was most probably due to different Ag NPs tested (commercial Ag NP
494 powder from Sigma-Aldrich).

495

496 ***Environmental implications***

497 Silver NPs are expected to enter the soil environment mainly via land application of
498 sewage sludge or biosolids, and also through direct application of products treated with Ag
499 NPs on compost heaps in gardens. Isopods can be found under stones and dead wood,
500 particularly in gardens, marginal grassland and open woodland. The concentrations of Ag NPs
501 tested in this work (10, 100, and 1000 mg Ag/kg of dry leaf mass) are higher than predicted
502 environmental values reported for soils treated with sludge (0.01–0.1 mg/kg; Gottschalk et al.,
503 2013), but the continuous input of biosolids to agricultural land may lead to increasing Ag NP
504 concentrations over time (Tourinho et al., 2015).

505 It is of particular interest that labile Ag-PVP complexes proved to be a source of
506 bioaccessible Ag to isopods. From an environmental safety perspective the PVP may not be
507 considered as the most suitable stabilizer of Ag NP suspensions. Although PVP does prevent
508 the aggregation of Ag NPs, the PVP-stabilized Ag NP suspensions have been shown to
509 contain high amounts of Ag-PVP complexes and free Ag⁺ content in total, i.e. 36.5 %
510 (Bondarenko et al., 2013), >40 % (Cunningham et al., 2013) or 46 % (Jemec et al 2016) for
511 suspensions prepared by different protocols. On the other hand, suspensions of uncoated Ag
512 NPs (Bondarenko et al., 2013) or Ag NPs coated with casein (Bondarenko et al., 2013) or
513 citrate (Ivask et al., 2014b) in deionized water were shown to contain much lower shares of
514 free Ag⁺ and/or Ag-ligand complexes, in the range of 0.82–7.6 %. The dissolution of various
515 Ag NPs (uncoated or coated with citrate, PVP, gelatin, 6-mercaptohexanoic acid or an
516 unspecified hydrophilic polymer) in the zebrafish hatching medium was in the range of 15–48
517 % after 120 h; the highest values were again reached by the PVP-stabilized Ag NPs
518 (Cunningham et al., 2013). The differences in the dissolution rates of variously-coated Ag
519 NPs might depend on the potential of the stabilizers to cause NP dissolution (Bondarenko et
520 al., 2013). Another reason for high Ag⁺ content in these suspensions might be the fact that Ag
521 NPs are often synthesized by the reduction of Ag⁺ to Ag⁰, so Ag⁺ might be the remnants from

522 the synthesis step if the NP suspension was not sufficiently purified (Koch et al., 2012). In the
523 latter case, the amount of free Ag^+ in the suspension depends on the stability of complexes
524 between Ag^+ and the NP-stabilizing compounds and on the amount of the stabilizer. We can
525 speculate that PVP in this way acts as a carrier for labile Ag^+ by forming weak coordinative
526 bonds with Ag^+ (Zhang et al., 1996; Wang et al., 2005).

527 In conclusion, we showed that terrestrial isopods are able to accumulate Ag from three
528 different Ag-species present in a composite Ag NP suspension: free Ag^+ , Ag-PVP complexes
529 and Ag NPs. The concentration of free Ag^+ in the suspension offered to the test organism is
530 not the only measure of bioavailable Ag. The data show that also the type of NP stabilizer
531 along with transformations in the digestive system need to be considered when the
532 bioavailability of metals from metal NPs is in question. This knowledge should be taken into
533 consideration in the creation of new computational models in nanomaterial fate evaluations.

534

535 **SUPPLEMENTARY MATERIAL**

536 The DLS analysis of supernatants of the Ag NP suspensions after ultracentrifugation.
537 The response of the Ag-ISE to the additions of Ag^+ standard to deionized water or to the
538 supernatants of the Ag NP suspensions. Scanning electron micrographs of Ag NP-spiked
539 hazelnut leaves before the experiment and the isopod fecal pellets after the experiment. The
540 feeding rate of the isopods fed with AgNO_3 -spiked or Ag NP-spiked food for 14 days. The
541 bioaccumulation of different Ag species from AgNO_3 -spiked or Ag NP-spiked food.
542 Equations used. Supplementary references.

543

544 **ACKNOWLEDGMENTS**

545 The paper is part of the PhD work of Tea Romih, working under the supervision of
546 Professor Damjana Drobne. The investigation was supported by the Ministry of Education,

547 Science and Sport of the Republic of Slovenia by a grant entitled “Innovative scheme of co-
548 funding doctoral studies for promoting co-operation with the economy and solving
549 contemporary social challenges” [Grant Number 1291]. This research also received funding
550 from the Slovenian Research Agency (ARRS) [Grant Agreements No. J1-4109 and P1-0034];
551 from the EU FP7 Project “NANOVALID” [Contract No. 263147]; and from the NanoFASE
552 Project [Grant Agreement No. 6460020] within the EU Horizon 2020 research and innovation
553 program. The results of this publication reflect only the author's view; the EU Commission is
554 not responsible for any use of the information it contains that may occur. The authors would
555 like to thank Dr. Matejka Podlogar from Jožef Stefan Institute for granting us access to the
556 scanning electron microscope.

557 **REFERENCES**

- 558 Beckman Coulter, 2007. Rotors and Tubes for Beckman Coulter Preparative Ultracentrifuges.
559 User's Manual No. LR-IM-24. Beckman Coulter, Inc., Brea, California, USA.
- 560 Bellanger, X., Billard, P., Schneider, R., Balan, L., Merlin, C., 2015. Stability and toxicity of
561 ZnO quantum dots: Interplay between nanoparticles and bacteria. *J. Hazard. Mater.* 283,
562 110–116.
- 563 Böhme, S., Stärk, H.J., Reemtsma, T., Kühnel, D., 2015. Effect propagation after silver
564 nanoparticle exposure in zebrafish (*Danio rerio*) embryos: a correlation to internal
565 concentration and distribution patterns. *Environ. Sci. Nano* 2, 603–614.
- 566 Bondarenko, O., Ivask, A., Käkinen, A., Kurvet, I., Kahru, A., 2013. Particle-cell contact
567 enhances antibacterial activity of silver nanoparticles. *PLOS ONE* 8, e64060.
- 568 Coutris, C., Joner, E.J., Oughton, D.H., 2012. Aging and soil organic matter content affect the
569 fate of silver nanoparticles in soil. *Sci. Total Environ.* 420, 327–333
- 570 Cunningham, S., Brennan-Fournet, M.E., Ledwith, D., Byrnes, L., Joshi, L., 2013. Effect of
571 nanoparticle stabilization and physicochemical properties on exposure outcome: acute
572 toxicity of silver nanoparticle preparations in zebrafish (*Danio rerio*). *Environ. Sci.*
573 *Technol.* 47, 3883–3892.
- 574 De Marco, R.; Clarke, G.; Pejcic, B., 2007. Ion-Selective Electrode Potentiometry in
575 Environmental Analysis. *Electroanalysis* 19, 1987–2001.
- 576 Diez-Ortiz, M., Lahive, E., Kille, P., Powell, K., Morgan, A.J., Jurkschat, K., van Gestel,
577 C.A.M., Mosselmans, J.F.W., Svendsen, C., Spurgeon, D.J., 2015. Uptake routes and
578 toxicokinetics of silver nanoparticles and silver ions in the earthworm *Lumbricus*
579 *rubellus*. *Environ. Toxicol. Chem.* 43, 2263–2270.
- 580 Dimeski, G., Badrick, T., John, A.S., 2010. Ion selective electrodes (ISEs) and
581 interferences—a review. *Clin. Chim. Acta*, 411, 309–317.

582 Domingos, R.F., Franco, C., Pinheiro, J.P., 2013. Stability of core/shell quantum dots—role
583 of pH and small organic ligands. *Environ. Sci. Pollut. Res.* 20, 4872–4880.

584 Domingos, R.F., Franco, C., Pinheiro, J.P., 2015. The role of charged polymer coatings of
585 nanoparticles on the speciation and fate of metal ions in the environment. *Environ. Sci.*
586 *Pollut. Res.* 22, 2900–2906.

587 Drobne, D., Hopkin, S.P., 1994. Ecotoxicological laboratory test for assessing the effects of
588 chemicals on terrestrial isopods. *Bull. Environ. Contam. Toxicol.* 53, 390–397.

589 Golobič, M., Jemec, A., Drobne, D., Romih, T., Kasemets, K., Kahru, A., 2012. Upon
590 exposure to Cu nanoparticles, accumulation of copper in the isopod *Porcellio scaber* is
591 due to the dissolved Cu ions inside the digestive tract. *Environ. Sci. Technol.* 46,
592 12112–12119.

593 Gottschalk, F., Sun, T.Y., Nowack, B., 2013. Environmental concentrations of engineered
594 nanomaterials: review of modeling and analytical studies. *Environ. Pollut.* 181, 287–300

595 Harris, D.C., 2010. *Quantitative Chemical Analysis*, 8th Edition. Palgrave Macmillan,
596 London.

597 He, X., Pan, Y., Zhang, J., Li, Y., Ma, Y., Zhang, P., Ding, Y., Zhang, J., Wu, Z., Zhao, Y.,
598 Chai, Z., Zhang, Z., 2015. Quantifying the total ionic release from nanoparticles after
599 particle–cell contact. *Environ. Pollut.* 196, 194–200.

600 Hames, C.A.C., Hopkin, S.P., 1989. The structure and function of the digestive system of
601 terrestrial isopods. *J. Zool.* 217, 599–627

602 Hopkin, S.P., 1990. Critical concentrations, pathways of detoxification and cellular
603 ecotoxicology of metals in terrestrial arthropods. *Funct. Ecol.* 4, 321–327.

604 Huynh, K.A., McCaffery, J.M., Chen, K.L., 2014. Heteroaggregation reduces antimicrobial
605 activity of silver nanoparticles: evidence for nanoparticle–cell proximity effects.
606 *Environ. Sci. Technol. Lett.* 1, 361–366.

607 Ivask, A., Juganson, K., Bondarenko, O., Mortimer, M., Aruoja, V., Kasemets, K., Blinova, I.,
608 Heinlaan, M., Slaveykova, V., Kahru, A., 2014a. Mechanisms of toxic action of Ag,
609 ZnO and CuO nanoparticles to selected ecotoxicological test organisms and mammalian
610 cells in vitro: A comparative review. *Nanotoxicology* 8, 57–71.

611 Ivask, A., Kurvet, I., Kasemets, K., Blinova, I., Aruoja, V., Suppi, S., Vija, H., Käkinen, A.,
612 Titma, T., Heinlaan, M., Visnapuu, M., Koller, D., Kisand, V., Kahru, A., 2014b. Size-
613 dependent toxicity of silver nanoparticles to bacteria, yeast, algae, crustaceans and
614 mammalian cells in vitro. *PLOS ONE* 9, e102108.

615 Jemec, A., Kahru, A., Potthoff, A., Drobne, D., Heinlaan, M., Böhme, S., Geppert, M.,
616 Novak, S., Schirmer, K., Rohit, R., Singh, S., Aruoja, V., Sihtmäe, M., Juganson, K.,
617 Käkinen, A., Kühnel, D., 2016. An interlaboratory comparison of nanosilver
618 characterisation and hazard identification: harmonising techniques for high quality data.
619 *Environ. Int.* 87, 20–32.

620 Koch M., Kiefer S., Cavellius C., Kraegeloh A., 2012. Use of a silver ion selective electrode to
621 assess mechanisms responsible for biological effects of silver nanoparticles. *J.*
622 *Nanopart. Res.* 14, 646–657.

623 Leclerc, S., Wilkinson, K.J., 2014. Bioaccumulation of Nanosilver by *Chlamydomonas*
624 *reinhardtii*. Nanoparticle or the Free Ion? *Environ. Sci. Technol.* 48, 358–364.

625 Lowry, G.V., Gregory, K.B., Apte, S.C., Lead, J.R., 2012. Transformations of nanomaterials
626 in the environment. *Environ. Sci. Technol.* 46, 6893–6899.

627 Merdzan, V., Domingos, R.F., Monteiro, C.E., Hadioui, M., Wilkinson, K.J., 2014. The
628 effects of different coatings on zinc oxide nanoparticles and their influence on
629 dissolution and bioaccumulation by the green alga, *C. reinhardtii*. *Sci. Total Environ.*
630 488, 316–324.

631 Misra, S.K., Dybowska, A., Berhanu, D., Luoma, S.N., Valsami-Jones, E., 2012. The
632 complexity of nanoparticle dissolution and its importance in nanotoxicological studies.
633 Sci. Total Environ. 438, 225–232.

634 Mu, Q., David, C.A., Galceran, J., Rey-Castro, C., Krzemiński, Ł., Wallace, R., Bamiduro, F.,
635 Milne, S.J., Hondow, N.S., Brydson, R., Vizcay-Barrena, G., Routledge, M.N., Jeuken,
636 L.J.C., Brown A.P., 2014. Systematic Investigation of the Physicochemical Factors That
637 Contribute to the Toxicity of ZnO Nanoparticles. Chem. Res. Toxicol. 27, 558–567.

638 Novak, S., Drobne, D., Golobič, M., Zupanc, J., Romih, T., Gianoncelli, A., Kiskinova, M.,
639 Kaulich, B., Pelicon, P., Vavpetič, P., Jeromel, L., Ogrinc, N., Makovec, D. 2013.
640 Cellular Internalization of Dissolved Cobalt Ions from Ingested CoFe₂O₄ Nanoparticles:
641 In Vivo Experimental Evidence. Environ. Sci. Technol. 47, 5400–5408.

642 Pesavento, M., Alberti, G., Biesuz, R., 2009. Analytical methods for determination of free
643 metal ion concentration, labile species fraction and metal complexation capacity of
644 environmental waters: A review. Anal. Chim. Acta 631, 129–141.

645 Pipan Tkalec, Ž., Drobne, D., Vogel-Mikuš, K., Pongrac, P., Regvar, M., Štrus, J., Pelicon, P.,
646 Vavpetič, P.; Grlj, N., Remškar, M., 2011. Micro-PIXE study of Ag in digestive glands
647 of a nano-Ag fed arthropod (*Porcellio scaber*, Isopoda, Crustacea). Nucl. Instr. Meth.
648 Phys. Res. B 269, 2286–2291.

649 Riding, M.J., Doick, K.J., Martin, F.L., Jones, K.C., Semple, K.T., 2013. Chemical measures
650 of bioavailability/bioaccessibility of PAHs in soil: fundamentals to application. J.
651 Hazard. Mater. 261, 687–700.

652 Romih, T., Drašler, B., Jemec, A., Drobne, D., Novak, S., Golobič, M., Makovec, D., Susič,
653 R., Kogej, K. 2015. Bioavailability of cobalt and iron from citric-acid-adsorbed
654 CoFe₂O₄ nanoparticles in the terrestrial isopod *Porcellio scaber*. Sci. Total Environ.
655 508, 76–84.

656 Romih, T., Hočevár, S.B., Jemec, A., Drobne, D., 2016. Bismuth film electrode for anodic
657 stripping voltammetric measurement of silver nanoparticle dissolution. *Electrochim.*
658 *Acta* 188, 393–397.

659 Shoults-Wilson, W.A., Reinsch, B.C., Tsyusko, O.V., Bertsch, P.M., Lowry, G.V., Unrine,
660 J.M., 2011. Effect of silver nanoparticle surface coating on bioaccumulation and
661 reproductive toxicity in earthworms (*Eisenia fetida*). *Nanotoxicology* 5, 432–444.

662 Schaumann, G.E., Philippe, A., Bundschuh, M., Metreveli, G., Klitzke, S., Rakcheev, D.,
663 Grün, A., Kumahor, S.K., Kühn, M., Baumann, T., Lang, F., Manz, W., Schulz, R.,
664 Vogel, H.J., 2015. Understanding the fate and biological effects of Ag- and TiO₂-
665 nanoparticles in the environment: The quest for advanced analytics and interdisciplinary
666 concepts. *Sci. Total Environ.* 535, 3–19.

667 Tantra, R., Bouwmeester, H., Bolea, E., Rey-Castro, C., David, C.A., Dogné, J.M., Jarman, J.,
668 Laborda, F., Laloy, J., Robinson, K.N., Undas, A.K., van der Zande, M., 2016.
669 Suitability of analytical methods to measure solubility for the purpose of
670 nanoregulation. *Nanotoxicology* 10, 173–184.

671 Tourinho, P.S., van Gestel, C.A.M., Jurkschat, K., Soares, A.M., Loureiro, S., 2015. Effects
672 of soil and dietary exposures to Ag nanoparticles and AgNO₃ in the terrestrial isopod
673 *Porcellionides pruinosus*. *Environ. Pollut.* 205, 170–177.

674 Tourinho, P.S., van Gestel, C.A.M., Morgan, A.J., Kille, P., Svendsen, C., Jurkschat, K.,
675 Mosselmans, J.F.W., Soares, A.M.V.M., Loureiro, S., 2016. Toxicokinetics of Ag in the
676 terrestrial isopod *Porcellionides pruinosus* exposed to Ag NPs and AgNO₃ via soil and
677 food. *Ecotoxicology* 25, 267–278.

678 Vijver M. G., Wolterbeek H. T., Vink J. P., van Gestel C. A. M. 2005. Surface adsorption of
679 metals onto the earthworm *Lumbricus rubellus* and the isopod *Porcellio scaber* is
680 negligible compared to absorption in the body. *Sci. Total. Environ.* 340, 271–280.

681 Wang, H., Qiao, X., Chen, J., Wang, X., Ding, S., 2005. Mechanisms of PVP in the
682 preparation of silver nanoparticles. *Mater. Chem. Phys.* 94, 449–453.

683 Zhang, Z., Zhao, B., Hu, L., 1996. PVP protective mechanism of ultrafine silver powder
684 synthesized by chemical reduction processes. *J. Solid State Chem.* 121, 105–110.

685 Zidar, P., Drobne, D., Štrus, J., 1998. Determination of moult stages of *Porcellio scaber*
686 (Isopoda) for routine use. *Crustaceana* 71, 646–654.

687 Zidar, P., Drobne, D., Štrus, J., Blejec, A., 2003. Intake and assimilation of zinc, copper, and
688 cadmium in the terrestrial isopod *Porcellio scaber* Latr.(Crustacea, Isopoda). *Bull.*
689 *Environ. Contam. Toxicol.* 70, 1028–1035.

690 Zimmer, M., Topp, W., 1997. Homeostatic responses in the gut of *Porcellio scaber* (Isopoda:
691 Oniscidea) optimize litter degradation. *J. Comp. Physiol. B.* 167, 582–585.

692 Zimmer, M., Brune, A., 2005. Physiological properties of the gut lumen of terrestrial isopods
693 (Isopoda: Oniscidea): adaptive to digesting lignocellulose? *J. Comp. Physiol. B.* 175,
694 275–283.

695 Zou, J., Hannula, M., Misra, S., Feng, H., Labrador, R.H., Aula, A.S., Hyttinen, J., Pyykkö, I.,
696 2015. Micro CT visualization of silver nanoparticles in the middle and inner ear of rat
697 and transportation pathway after transtympanic injection. *J. Nanobiotechnol.* 13, 1–9.

698

699 **TABLES WITH CAPTIONS**

700

701 **Table 1.** The total concentration of Ag in Ag NP suspensions, measured by atomic absorption spectrometry (AAS); the concentrations of Ag-PVP complexes and free Ag⁺,
 702 measured by anodic stripping voltammetry (ASV); and the concentrations of free Ag⁺ only, measured by potentiometry with the silver ion-selective electrode (Ag-ISE). The
 703 values measured by AAS correspond to acidified samples, whereas the ASV and potentiometric measurements were performed without prior acidification.

Nominal Ag concentration in the Ag NP suspensions (mg/L)	AAS-measured Ag concentration in the Ag NP suspensions (mg/L), mean ± SD (n = 3)	Concentration of Ag in the supernatants (mg/L; mean ± SD)			The average share of Ag in the supernatants (%) ^a		
		Total Ag (free Ag ⁺ , Ag- PVP complexes and Ag NPs), AAS (n = 3)	Free Ag ⁺ and Ag-PVP complexes, ASV (n = 2)	Free Ag ⁺ , potentiometry (n = 2)	Total Ag (free Ag ⁺ , Ag-PVP complexes and Ag NPs), AAS	Free Ag ⁺ and Ag-PVP complexes, ASV	Free Ag ⁺ , potentiometry
12.5	10.6 ± 0.1	5.25 ± 0.03	4.5 ± 0.2	2.86 ± 0.07	50	42	27
25	20.9 ± 0.9	11.0 ± 0.1	9.9 ± 0.5	2.5 ± 0.3	53	47	12
50	44.9 ± 1.1	23.6 ± 0.1	19.9 ± 0.2	5.4 ± 0.2	53	44	12 ^b

704 ^a, calculated in comparison to the AAS-quantified total Ag content of the suspensions from the corresponding average values.

705 ^b, the value may not be entirely accurate due to suboptimal electrode operation (details are provided in the **Supplementary Material, Figures S4 and S5**).

706 Ag NPs, silver nanoparticles; Ag-PVP complexes, complexes of silver with polyvinylpyrrolidone.; AAS, atomic absorption spectrometry; ASV, anodic stripping voltammetry;

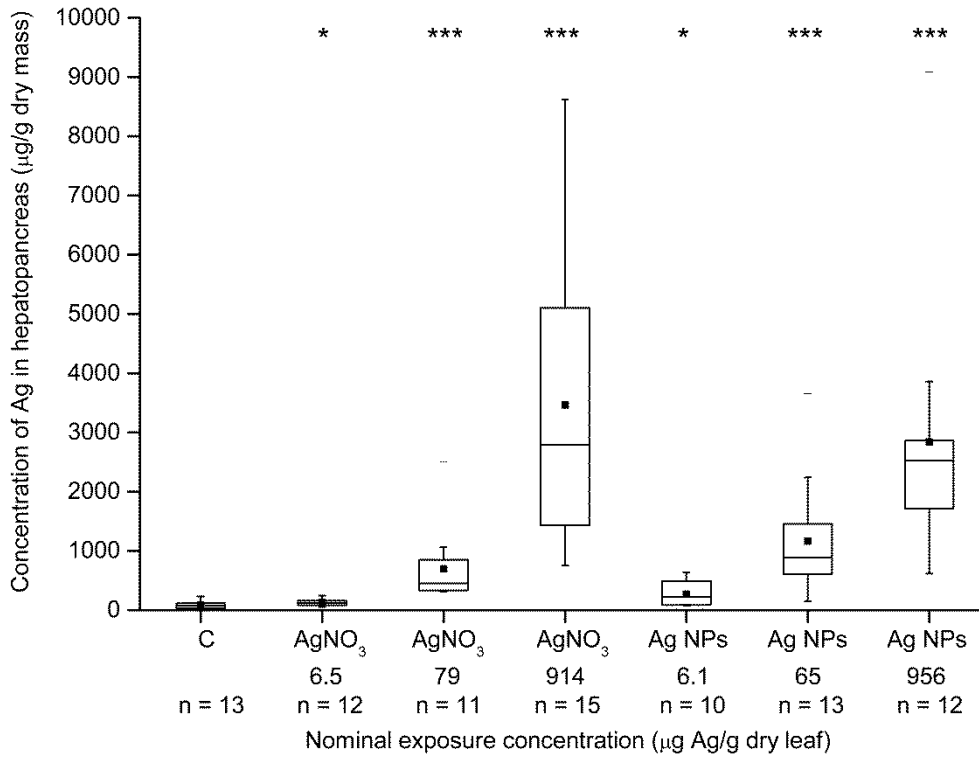
707 *n* = number of replicates; *SD* = standard deviation

708 **FIGURES WITH CAPTIONS**

709

710 **Figure 1**

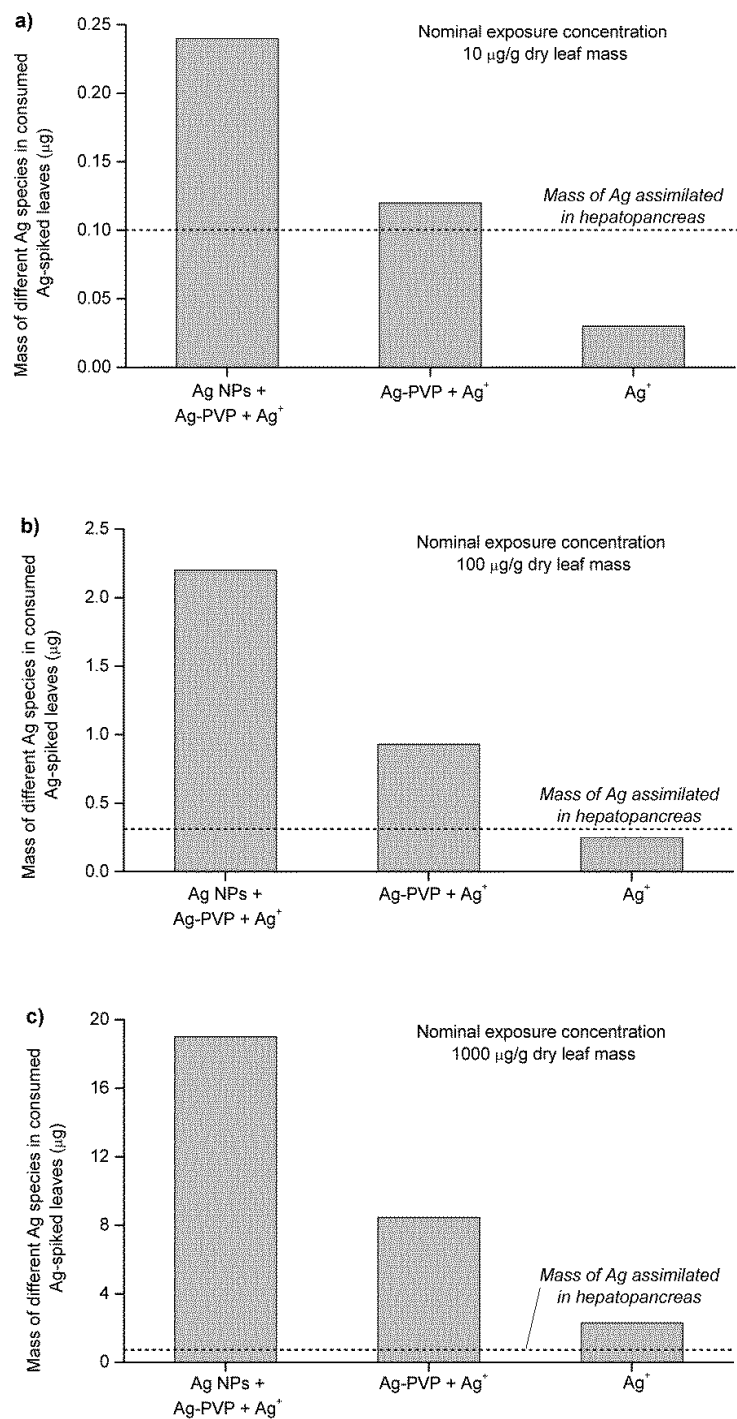
711



712

713 **Figure 1.** Concentrations of Ag in the digestive glands of isopods *P. scaber* after feeding for 14 days on Ag-
 714 spiked food. The animals were fed non-spiked food (control, C) or food that was spiked with AgNO₃ (nominally
 715 10, 100, and 1000 µg Ag/g of dry leaf mass) or Ag nanoparticles (Ag NPs; nominally 10, 100, and 1000 µg Ag/g
 716 of dry leaf mass). Actual measured exposure concentrations of Ag are provided on the x-axis. Symbols on the
 717 box plot represent maximum and minimum values (whiskers: ⊥), mean values (■), outliers (—), statistical
 718 differences between the control and the test groups with $p < 0.05$ (*) and $p < 0.001$ (***); n = number of
 719 specimens in each test group.

720



722

723 **Figure 2.** Comparison of the Ag mass found in the hepatopancreas (dashed line) after the experiment to the
 724 masses of each ingested Ag species as the potential source of bioaccumulated Ag from Ag NP suspension at
 725 exposure concentrations of a) 10, b) 100, c) 1000 µg Ag/g of dry food. The data represent the averages extracted
 726 from **Table S1, Supplementary Material**. Ag NPs, silver nanoparticles; Ag-PVP, complexes of silver with
 727 polyvinylpyrrolidone; Ag⁺, free silver ions.